

# A Density Functional Study of $[\text{Fe}(\text{PR}_3)_4\text{H}_3]^+$ Isomers: Comparing Model Compounds ( $\text{R} = \text{H}$ ) with Real Molecules ( $\text{R} = \text{CH}_3$ )

Heiko Jacobsen and Heinz Berke\*

**Abstract:** The structures, energetics, and dynamics of various isomers of  $[\text{Fe}(\text{PR}_3)_4\text{H}_3]^+$  ( $\text{R} = \text{H}, \text{Me}$ ) were studied by density functional theory. The conformations considered were derived from a square planar (P), tetrahedral (T) and  $C_{2v}$ -butterfly (C) arrangement of the phosphine ligands. For  $\text{PH}_3$ , the stability ranking  $\text{P} \approx \text{C} > \text{T}$  was obtained, whereas

in the  $\text{PMe}_3$  case the P isomer was least stable,  $\text{T} > \text{C} > \text{P}$ . Mechanisms for the hydrogen exchange in the C and T

isomers are discussed. For the latter, this process might be described as a tetrahedral jump, but could also be viewed as a dodecahedral distortion of a cubic arrangement. The theoretical findings are compared with the results of experimental studies of  $[\text{Fe}(\text{PR}_3)_4\text{H}_3]^+$  ( $\text{R} = \text{Me}, \text{Et}$ ).

## Keywords

density functional calculations · iron · ligand effects · molecular modeling · phosphorus

## Introduction

One of the important aspects of modern coordination chemistry is that of stereochemically nonrigid structures.<sup>[1]</sup> Research in this area has developed rapidly since the early sixties, and as far back as 30 years ago Muetterties pointed out that “the neglect of the effect of dynamics on stereochemistry can lead to serious misconceptions and, at the very least, is a step removed from reality”.<sup>[2]</sup>

The field of fluxional behavior of transition-metal hydrides was pioneered by Meakin, Muetterties, and co-workers, who studied the dynamics of the hydrogen exchange in a series of  $\text{MH}_2\text{L}_4$  complexes.<sup>[3]</sup> In connection with a mechanism for the process investigated, the term “tetrahedral jump” was coined, which—and it is very important to note this—was intended only to describe the shift of one H nucleus from an occupied to a vacant coordination site,<sup>[3d]</sup> and which should not be associated with any actual physical path.<sup>[3e]</sup>

Since then, a great deal of interest has been generated in the structure and dynamics of transition-metal hydride complexes,<sup>[4]</sup> including in the field of cationic complexes of the type  $[\text{MH}_3\text{L}_4]^+$ . Depending on the nature of the ligand and the respective transition metal, these compounds exhibit different coordination geometries.<sup>[5]</sup> Three prominent examples are the so-called P-, C-, and T-type structures (vide infra). Here, the P, C, and T nomenclature is derived from the coordination sphere of the ligands L, which are based on a square planar,  $C_{2v}$ -butterfly, or tetrahedral arrangement, respectively.<sup>[6]</sup>

In our laboratories, we recently characterized the structures and the dynamics of cationic Group VIII complexes of the type  $[\text{MH}_3\text{L}_4]^+$  ( $\text{M} = \text{Fe}, \text{Ru}, \text{Os}$ ;  $\text{L} = \text{PMe}_3, \text{PEt}_3$ ).<sup>[7]</sup> We now present the first results of a companion theoretical study, which was based on approximate density functional theory (DFT).<sup>[8]</sup> In the present paper, we report calculations on the isomers of  $[\text{FeH}_3(\text{PR}_3)_4]^+$  ( $\text{R} = \text{H}, \text{Me}$ ). Three problems constitute the main focus of this work. Firstly, we wanted to investigate the structures and relative energies of several isomers. While the results of this investigation support our interpretation of experimental findings for  $[\text{FeH}_3(\text{PR}_3)_4]^+$ , a broader concern (and the second aspect of our work) is the validity of the theoretical approach. A wide variety of calculations on transition-metal hydride complexes exists in the literature,<sup>[9]</sup> in which very often the  $\text{PR}_3$  ligands are modelled by  $\text{PH}_3$ . The validity of the model was first analyzed by Lin and Hall<sup>[10]</sup> in connection with the problem of classical and nonclassical isomers of  $[\text{IrH}_5\text{L}_2]$ . The authors concluded that the replacement is a reasonable choice for this particular field of calculations. Our results, however, indicate that this approximation has to be abandoned when the electronic structure of the metal complex is mainly determined by phosphorus donor ligands. Lastly, we try to establish possible descriptions for the hydrogen exchange in the C-type and T-type structures. We will present a concise description of our computational approach before discussing our results in more detail.

## Computational Methods

**General procedure:** All calculations were based on the local density approximation (LDA) in the parametrization of Vosko, Wilk, and Nussair,<sup>[11]</sup> with the addition of the gradient corrections of Becke<sup>[12]</sup> and Perdew<sup>[13]</sup> (GGA). The GGA was included self-consistently (NL-SCF). The calculations utilized

[\*] H. Berke, H. Jacobsen  
Anorganisch-Chemisches Institut der Universität Zürich  
Winterthurerstr. 190, CH-8057 Zürich (Switzerland)  
Fax: Int. Code + (1) 364-0191  
e-mail: hberke@aci.unizh.ch

the Amsterdam Density Functional package (ADF) release 2.0.1.<sup>[14]</sup> Use was made of the frozen core approximation. For C and P, the valence shells were described by a double  $\zeta$ -STO basis, augmented by one  $d$ -STO polarization function (ADF database III). For the  $ns$ ,  $np$ ,  $nd$ ,  $(n+1)s$ , and  $(n+1)p$  shells on Fe, a triple  $\zeta$ -STO basis was employed (ADF database IV, augmented by  $\alpha_{4p} = 0.90$ , 1.40, and 2.30). H was treated with a double  $\zeta$ -STO basis and one additional  $p$ -STO polarization function (ADF database III). The numerical integration grid was chosen such that significant test integrals are evaluated with an accuracy of at least four significant digits. No symmetry constraints were applied in the calculations. All molecules were fully optimized at the quantum mechanical level.

**Energy analysis:** The total bonding energy (TBE), which is associated with the formation of a molecule from its atomic fragments, can be expressed as in Equation (1),<sup>[15]</sup> where  $\Delta E^0$  is steric repulsion and  $\Delta E_{\text{int}}$  is orbital interaction. The term  $\Delta E^0$  consists of two components [Eq. (2)]. Here,

$$\text{TBE} = \Delta E^0 + \Delta E_{\text{int}} \quad (1)$$

$$\Delta E^0 = \Delta E_{\text{elstat}} + \Delta E_{\text{pauli}} \quad (2)$$

$\Delta E_{\text{elstat}}$  describes the pure Coulomb interaction between the atomic fragments, and it is usually attractive. The term  $\Delta E_{\text{pauli}}$ , which is called exchange repulsion or Pauli repulsion, takes into account the destabilizing two-orbital three- or four-electron interactions between occupied orbitals. The second term on the right-hand side of Equation (1),  $\Delta E_{\text{int}}$ , includes the attractive orbital interactions.

**Charge analysis:** Atomic charges are evaluated by a Hirshfeld charge analysis.<sup>[16]</sup> In this approach, the total electronic charge in a bonded atom  $i$  is given as expressed in Equation (3). Here  $\rho_i^{\text{at}}$  describes an initial atomic density,

$$Q_i = - \int \frac{\rho_i^{\text{at}}(\mathbf{r})}{\sum_j \rho_j^{\text{at}}(\mathbf{r})} \cdot \rho^{\text{mol}}(\mathbf{r}) d\mathbf{r} \quad (3)$$

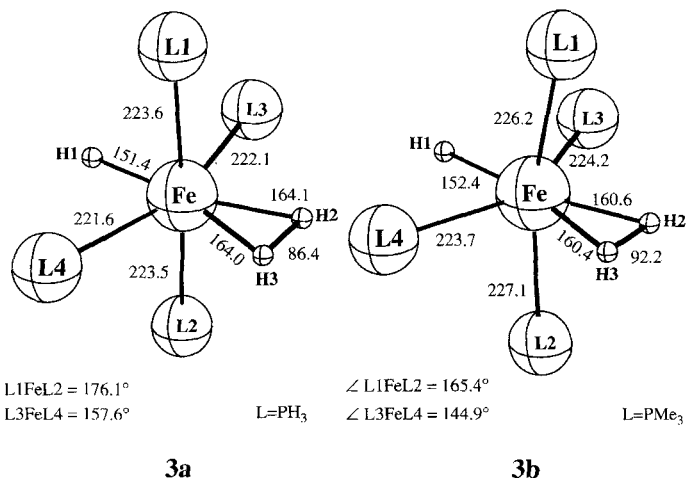
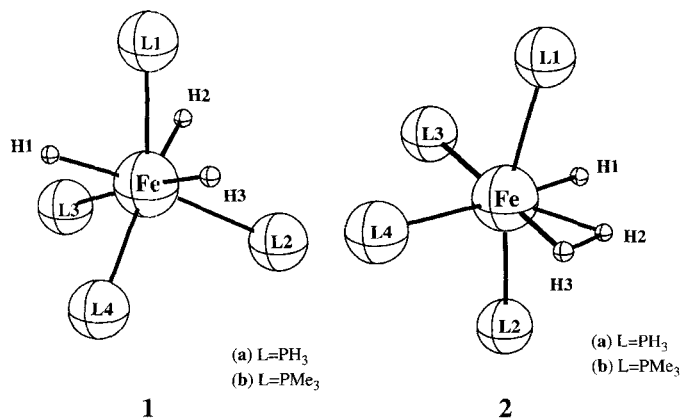
density, whereas  $\rho^{\text{mol}}$  is the molecular density, obtained as the result of the self-consistent calculation. Adding the nuclear charge  $Z_i$  gives the net atomic charge  $q_i$  [Eq. (4)]. Hirshfeld net atomic charges define the reorganization

$$q_i = Q_i + Z_i \quad (4)$$

of charge taking place when the atomic fragments, placed on their appropriate positions, interact to form the actual molecule.

## Results and Discussion

We begin our discussion with calculations on the T, C, and P isomers of  $[\text{Fe}(\text{PH}_3)_4\text{H}_3]^+$  (**1a**, **2a**, **3a**) as well as on  $[\text{Fe}(\text{PMe}_3)_4\text{H}_3]^+$  (**1b**, **2b**, **3b**). Before we analyze energetic differences between the isomers as well as possible mechanisms for the H-exchange process in **1b** and **2b**, we will briefly comment on the optimized geometries in comparison with results obtained from single-crystal studies.



**Structures of T, C, and P isomers of  $[\text{Fe}(\text{PR}_3)_4\text{H}_3]^+$  systems:** The structure of the T-type isomers is shown in **1**. Selected optimized bond lengths and bond angles, together with the corresponding data from an X-ray analysis of  $[\text{Fe}(\text{PEt}_3)_4\text{H}_3]^+$ , are collected in Table 1. The T-type isomers possess a pseudo- $C_3$  symmetry axis,

Table 1. Comparison of selected geometrical parameters (distances in pm, angles in  $^\circ$ ) for the X-ray structure [a] of T- $[\text{Fe}(\text{PEt}_3)_4\text{H}_3]^+$  and the calculated [b] structures of T- $[\text{Fe}(\text{PR}_3)_4\text{H}_3]^+$  (R = H (**1a**), Me (**1b**)).

	T- $[\text{Fe}(\text{PEt}_3)_4\text{H}_3]^+$ , X-ray	<b>1b</b> , DFT	<b>1a</b> , DFT
$d(\text{Fe}-\text{H})$ [c]	144(7)	152.2	152.7
$d(\text{Fe}-\text{P}1)$	217.0	214.6	214.5
$d(\text{Fe}-\text{P}2,3,4)$ [c]	228.1	225.6	223.5
$\angle (\text{P}1-\text{Fe}-\text{P}2)$	122.2	119.4	121.7
$\angle (\text{P}1-\text{Fe}-\text{P}3)$	117.4	117.8	117.3
$\angle (\text{P}1-\text{Fe}-\text{P}4)$	113.8	118.4	116.9
$\angle (\text{P}2-\text{Fe}-\text{P}3)$	96.5	98.7	97.5
$\angle (\text{P}3-\text{Fe}-\text{P}4)$	101.5	99.6	98.6
$\angle (\text{P}4-\text{Fe}-\text{P}2)$	102.1	98.8	101.3

[a] Ref. [7]. [b] This work. [c] Averaged value.

which lies along the Fe–P1 bond. The calculations are able to reproduce the fact that this distinct Fe–P bond is 11 pm shorter than the other Fe–P distances. In general, the calculated Fe–P lengths are only about 2 pm (**1b**) to 4 pm (**1a**) shorter than those measured for the analogous  $[\text{Fe}(\text{PEt}_3)_4\text{H}_3]^+$  structure. The theoretical Fe–H distances match the crystal structure within experimental error. Compared with the excellent agreement in the bond lengths, the deviation between calculated and experimentally observed angles is somewhat larger. However, both experiment and theory indicate that P–Fe–P angles that involve the P1 ligand are opened up by about  $10^\circ$  compared to an ideal tetrahedron, whereas the values for other P–Fe–P angles are about  $10^\circ$  smaller than in the ideal case. Overall, the two calculated structures **1a** and **1b** are in very good agreement with the experimental results.

We next turn to the C-type isomers, for which the geometric arrangement is displayed in structure **2**. Values for bond lengths and bond angles are presented in Table 2. Also included are geometric parameters for  $[\text{Fe}(\text{PMe}_3)_4\text{H}_3]^+$  in the crystal. Once again, we note the excellent agreement between theoretical and

Table 2. Comparison of selected geometrical parameters (distances in pm, angles in °) for the X-ray [a] and calculated [b] structures of C- $[\text{Fe}(\text{PR}_3)_4\text{H}_3]^+$  (R = H (**2a**), Me (**2b**)).

	C- $[\text{Fe}(\text{PMe}_3)_4\text{H}_3]^+$ , X-ray	<b>2b</b> , DFT	<b>2a</b> , DFT
$d(\text{Fe}-\text{H}1)$	148(3)	151.7	152.9
$d(\text{Fe}-\text{H}2)$	153(4)	156.4	157.1
$d(\text{Fe}-\text{H}3)$	172(4)	159.8	160.2
$d(\text{H}2-\text{H}3)$	84(4)	90.7	90.4
$d(\text{Fe}-\text{P}1)$	223.0(1)	224.9	223.4
$d(\text{Fe}-\text{P}2)$	223.1(1)	226.4	223.2
$d(\text{Fe}-\text{P}3)$	221.2(1)	224.6	221.2
$d(\text{Fe}-\text{P}4)$	226.0(1)	227.5	224.8
$\angle(\text{H}1-\text{Fe}-\text{H}2)$	76(2)	67.6	68.7
$\angle(\text{P}1-\text{Fe}-\text{P}2)$	152.51(3)	158.2	165.2
$\angle(\text{P}1-\text{Fe}-\text{P}3)$	95.59(3)	92.9	91.9
$\angle(\text{P}2-\text{Fe}-\text{P}3)$	98.05(3)	93.4	91.9
$\angle(\text{P}3-\text{Fe}-\text{P}4)$	94.0	101.6	97.8

[a] Ref. [7]. [b] This work.

experimental bond lengths. In particular, calculations and experiment are consistent in that the P ligand in the *trans* position to the H1 ligand forms the longest Fe–P bond, whereas the P ligand *trans* to the H2–H3 dihydrogen ligand shows the shortest Fe–P separation. Two of the Fe–H distances are well represented in the calculations, whereas the experimental and theoretical values for  $d_{\text{Fe}-\text{H}3}$  differ by 12 pm. In the crystal structure, the H<sub>2</sub> ligand is asymmetrically coordinated to the metal fragment, with Fe–H distances differing by 20 pm. In the optimized structure, the H<sub>2</sub> ligand is nearly symmetrically bonded to the iron center, the distances Fe–H2 and Fe–H3 differing only by 3 pm. These differences in the H<sub>2</sub> coordination are also reflected in the discrepancies of the actual and calculated angles, involving the relevant ligands. Overall, and also in view of the high standard deviations of the hydrogen positions in the X-ray diffraction study, the calculated and the experimentally determined geometries for the C-type structures are in good agreement.

The last set of isomers that we include in our discussion are P- $[\text{Fe}(\text{PH}_3)_4\text{H}_3]^+$  and P- $[\text{Fe}(\text{PMe}_3)_4\text{H}_3]^+$ . The optimized geometries for these structures are displayed in **3a** and **3b**, respectively. Whereas in the case of the C- and T-type isomers structures involving PH<sub>3</sub> or PMe<sub>3</sub> ligands are very similar, we observe a significant ligand influence on the P-type geometries. In structure **3a**, the atoms P1, P2 exhibit a slight bend toward the hydride H1, forming an angle P1–Fe–P2 of 176°. In **3b**, on the other hand, the P1 and P2 ligands are now bent toward the dihydrogen ligand H2–H3, forming an angle P1–Fe–P2 of 165°. In  $[\text{Fe}(\text{PH}_3)_4\text{H}_3]^+$ , H2 and H3 are located about 164 pm away from the iron center; the H–H bond length amounts to 86 pm. On going to the PMe<sub>3</sub>-substituted species, a change in the arrangement of the coordinated dihydrogen ligand is observed. The Fe–H distance is now shorter by 4 pm, whereas  $d_{\text{H}-\text{H}}$  is increased by 6 pm. This is a first indication that the nature of the bond between the hydrogen ligands and the  $\text{Fe}(\text{PR}_3)_4$  fragment is indeed sensitive to the nature of the PR<sub>3</sub> ligand. It also suggests how the relative stability of the different isomers can be affected by a change of the phosphorus donor ligand. In the next section, we shall discuss the energetic differences and the bonding in the various isomers in more detail.

**Energy analysis:** The relative energies of the different isomers **1–3** are displayed in Figure 1. For  $[\text{Fe}(\text{PH}_3)_4\text{H}_3]^+$ , the

P-type **3a** and C-type **2a** isomers are very close in energy, the C-type being favored by 3 kJ mol<sup>-1</sup>. The T-type structure **1a**, at 35 kJ mol<sup>-1</sup>, lies considerably higher in energy than **2a**. Ab initio studies by Maseras and co-workers<sup>[17a]</sup> on the same molecule also predicted the P structure to be the isomer of lowest energy, but arrived at a considerably higher energetic difference of 46 kJ mol<sup>-1</sup> between the P- and C-type structures. A different energetic ranking is found where  $[\text{Fe}(\text{PMe}_3)_4\text{H}_3]^+$  is concerned. In this case, the T-type isomer **1b** becomes the most stable species. The C and P structures **2b** and **3b** are 11 kJ mol<sup>-1</sup> and 23 kJ mol<sup>-1</sup> higher in energy, respectively.

In NMR solution studies of  $[\text{Fe}(\text{PMe}_3)_4\text{H}_3]^+$  the C and T isomers were observed, and no indication for a P-type structure was found.<sup>[7]</sup> However, the experiment revealed that the two structures have the same enthalpy, the C-type structure being favored over the T-type by entropic effects.<sup>[7]</sup> When comparing the experimental and theoretical results, one should be aware of the fact that the calculations refer to single molecules in the gas phase. Different energies of solvation certainly affect the relative stabilities of the two isomers in solution. The experiment indicated that the C-type structure is better solvated in polar solvents, since the equilibrium constant  $K = [\text{C}, \mathbf{2b}]/[\text{T}, \mathbf{1b}]$  increased with increasing dielectric constant of the solvent.<sup>[7]</sup> The zero-point energies for **1b** and **2b** should be similar, since both isomers have the same number and type of bonds. One could expect the C isomer to show a somewhat higher zero-point energy, owing to the maintained H–H bond.

The Hirshfeld charge analysis, as presented in Table 3, provides a first explanation of the different stability ranking of the structures with PH<sub>3</sub> or PMe<sub>3</sub> ligands. In the T-type, the H ligands carry a negative charge. For the C structures the charge for hydride ligand H1 is negative, whereas the dihydrogen ligand H2–H3 carries a positive charge. This indicates that the H<sub>2</sub>

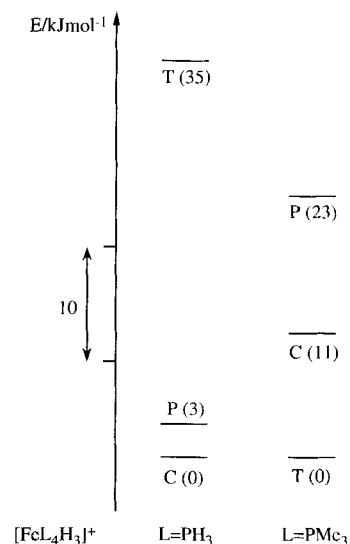


Figure 1. Relative energies of the T, C, and P isomers of  $[\text{Fe}(\text{PMe}_3)_4\text{H}_3]^+$  and  $[\text{Fe}(\text{PH}_3)_4\text{H}_3]^+$ .

Table 3. Hirshfeld charge analysis (a.u.) for three isomers of  $[\text{Fe}(\text{PR}_3)_4\text{H}_3]^+$  (R = H, Me).

	$[\text{Fe}(\text{PH}_3)_4\text{H}_3]^+$			$[\text{Fe}(\text{PMe}_3)_4\text{H}_3]^+$		
	T, <b>1a</b>	C, <b>2a</b>	P, <b>3a</b>	T, <b>1b</b>	C, <b>2b</b>	P, <b>3b</b>
Fe	-0.185	-0.169	-0.167	-0.182	-0.172	-0.173
H1	-0.037	-0.052	-0.066	-0.049	-0.060	-0.067
H2	-0.035	0.012	0.009	-0.049	0.009	-0.006
H3	-0.037	0.023	0.008	-0.049	0.001	-0.007
P1	0.282	0.236	0.230	0.334	0.304	0.305
P2	0.231	0.236	0.232	0.303	0.306	0.304
P3	0.231	0.220	0.227	0.303	0.296	0.297
P4	0.226	0.197	0.228	0.301	0.278	0.298

ligand is mainly bonded by  $\sigma$  donation. It also suggests that the T-type structure is stabilized by more electron-rich metal centers, and thus by coligands which are good  $\sigma$  donors. For the C-type and P-type structures, the ability of the  $H_2$  ligand to compete with the phosphine ligands for  $\sigma$  donation becomes important.

If the phosphine ligands are good  $\sigma$  donors,<sup>[18]</sup> like for example  $PMe_3$ , one should expect hydride coordination to be favored over the dihydrogen case, and thus that the T isomer is favored over the C and P structures in terms of the bonding of the hydrogens to the metal center. Turning to a weak  $\sigma$  donor like  $PH_3$ ,<sup>[18]</sup> the  $H_2$  ligand can successfully compete with the phosphine for  $\sigma$  donation, and the C and P isomers gain in stability compared to the T isomer.

It is of further interest to note that in all cases the iron centers carry about the same amount of negative charge. This indicates that donation from the P ligand to the Fe center is the dominant bonding interaction for all the isomers. The formal change of the oxidation number at the Fe center between the C-type ( $Fe^{II}$ ) to T-type structure ( $Fe^{IV}$ ) does not provide an obvious explanation for the difference in stability.<sup>[20]</sup> It is rather the distinct nature of the hydrogen ligands that is responsible for energetic differences.

The results of the bonding analysis are presented in Table 4. The energies and their contributions are given relative to the T-type isomers. Negative values indicate stabilization, positive destabilization. If we compare the C and T isomers, we find in both cases ( $L = PH_3, PMe_3$ ) that the C structures **2** exhibit about  $210 \text{ kJ mol}^{-1}$  less steric repulsion than the T structures **1**.

Table 4. An analysis of the relative energies ( $\text{kJ mol}^{-1}$ ) for three isomers of  $[Fe(PR_3)_4H_3]^+$  ( $R = H, Me$ ). For the T isomer, the energy terms are set to zero in both cases.

	$[Fe(PH_3)_4H_3]^+$			$[Fe(PMe_3)_4H_3]^+$		
	T, <b>1a</b>	C, <b>2a</b>	P, <b>3a</b>	T, <b>1b</b>	C, <b>2b</b>	P, <b>3b</b>
$\Delta E^0$	0	-213	-182	0	-212	-375
$\Delta E_{int}$	0	178	150	0	223	398
TBE	0	-35	-32	0	11	23

The increase in steric repulsion on going from C to T is mainly determined by the arrangement of the hydrogens. Surprisingly, the different bulk of the phosphine ligands constitutes only a secondary effect. The average H–P distance in C-type geometries is about 250 pm. In the T type there are very short H–P1 contacts of 210 pm, giving rise to the increase in steric energy. On turning to the electronic interaction term, we realize that now the T structures, **1**, are favored over those of the C-type, **2**. One sees further that for  $L = PH_3$  this stabilization cannot overcome the increase in steric demand; thus the C structure of **2a** is more stable than the T structure of **1a**. However, introduction of the better electron donor  $L = PMe_3$  favors the T-type structure **1b**.

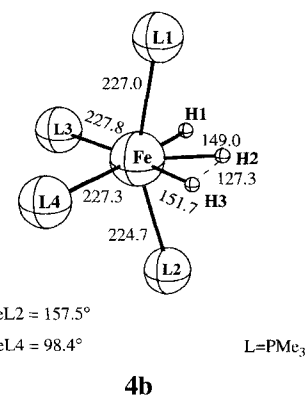
For the P-type isomers we observe more pronounced changes when going from  $PH_3$  to  $PMe_3$ . For **3b**, the steric stabilization and electronic destabilization compared with the T structures are both more than twice as large as for **3a**. This is a consequence of the significant differences in the geometry of **3a** and

**3b** (vide supra). It is again the fine balance between steric and electronic terms that is of importance for the relative energies of the P-type structures. As mentioned above, for  $[Fe(PMe_3)_4H_3]^+$  the P isomer is least favored on energetic grounds. However, the importance of the P-structure should not be underestimated, since many representatives of the  $[ML_4H_3]^+$  series ( $M = Fe, Ru, Os$ ), mainly those possessing bidentate phosphine ligands, prefer a P-type arrangement of the framework of the phosphine ligands.<sup>[51]</sup>

**A short comment on classical and nonclassical hydride complexes:** Nonclassical hydride complexes, which have been isolated by Kubas,<sup>[22]</sup> contain a dihydrogen ligand coordinated through  $\sigma$  donation, in contrast to the classical hydride complexes. So far we have discussed the nonclassical C- and P-type structures. One should consider the classical alternatives  $C_c$  and  $P_c$  as well. Studies by Li and Ziegler<sup>[23]</sup> on the related systems  $[M(PH_3)_3H_4]$  ( $M = Fe, Ru, Os$ ) indicate that nonclassical complexes are formed with Fe and Ru, whereas Os prefers the classical coordination. This result can be explained by relativistic effects. The  $C_c$  and the  $P_c$  isomers will however be of importance in the last sections of our discussion. An example for a  $P_c$ -type structure in the  $[ML_4H_3]$  series is the rhenium complex  $[ReH_3(CO)(PMe_3)_3]$ , for which we recently described the crystal structure.<sup>[24]</sup>

**Mechanism of the hydrogen exchange in C- $[Fe(PMe_3)_4H_3]^+$ :** The hydrogen exchange in C- $[Fe(PH_3)_4H_3]^+$  (**2a**) has been extensively studied by Maseras and coworkers.<sup>[17b]</sup> They found a transition-state structure for this process in which the central hydrogen atom is equidistant from the other two.<sup>[25]</sup> The H–H distance was calculated as 104 pm, and the two Fe–H separations were 156 pm for the central H atom and 167 pm for the remaining two hydrogen ligands. The activation barrier for H exchange was calculated to be  $13 \text{ kJ mol}^{-1}$ . We could locate a classical C-type structure as a possible transition state for the H exchange in  $Fe[(PMe_3)_4H_3]^+$  (**2b**). This  $C_c$ -isomer is shown in structure **4b**. The arrangement of the hydride ligands differs from that obtained by Maseras and coworkers for C- $[Fe(PMe_3)_4H_3]^+$  in that the H–H distance is about 20 pm longer, and the Fe–H contacts are 7–15 pm shorter. The arrangement of the phosphine ligands in **4b** is similar to that of the nonclassical isomer **2b**. The activation barrier for the hydrogen exchange with **4b** as transition-state structure amounts to only  $2 \text{ kJ mol}^{-1}$ . This corresponds well with the experimental fact that very fast H/ $H_2$  scrambling is observed even at temperatures as low as  $-140^\circ\text{C}$ .<sup>[7]</sup>

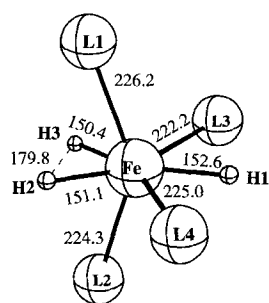
As seen above, the H exchange in the C isomer **2b** does not require a drastic rearrangement of the phosphine ligands, and is mainly determined by the motion of the H atoms. This is in



contrast to the mechanism for the T-type isomer (**1b**), which we discuss in the next section.

**Mechanism of the hydrogen exchange in T- $[\text{Fe}(\text{PMe}_3)_4\text{H}_3]^+$ :** The “tetrahedral jump” model has been suggested as a possible mechanism to describe the fluxional behavior of the hydrogen ligands in the T-type structure. The name “tetrahedral jump” might imply that during the exchange process only one hydrogen ligand is moving, keeping the frame of the phosphine ligand more or less rigid. This, however, is not the case. Muettterties and coworkers introduced this name just to emphasize the topological aspect that only one H atom is changing place during the process of isomerization. They further point out that their NMR work does not provide any mechanistic information to determine the actual physical path involved,<sup>[3c]</sup> and that in the particular case of  $[\text{FeH}_2(\text{PR}_3)_4]$  fluxionality the motion of the phosphorus ligands makes the major contribution to the reduced mass for the exchange process.<sup>[3d]</sup>

One of the requirements of the tetrahedral jump mechanism is that at some time during the process one H–Fe vector and two P–Fe vectors must be coplanar. A geometry optimization enforcing this constraint for  $[\text{Fe}(\text{PH}_3)_4\text{H}_3]^+$  led directly to the P-type structure. For  $[\text{Fe}(\text{PMe}_3)_4\text{H}_3]^+$  however, this optimization



$\angle \text{L1FeL2} = 144.9^\circ$

$\angle \text{L3FeL4} = 123.3^\circ$

**5b**

L=PMe<sub>3</sub>

resulted in a structure as shown in **5b**, which is a likely candidate for the transition-state structure of the H exchange in T- $[\text{Fe}(\text{PMe}_3)_4\text{H}_3]^+$ . Structure **5b** lies 31 kJ mol<sup>-1</sup> higher in energy than **1b**. This corresponds excellently with the experimentally obtained activation barrier of 33 kJ mol<sup>-1</sup>.<sup>[7]</sup> The relationship between the

different isomers of  $[\text{Fe}(\text{PMe}_3)_4\text{H}_3]^+$  is summarized in Figure 2. As mentioned above, the isomers C and T can be observed in NMR experiments, and do exchange. The P-type structure cannot be found. It is likely that the P isomer **3b** is related to the T structure (**1b**) via the transition state for the hydrogen exchange. It might be possible that **3b** constitutes a short-lived intermedi-

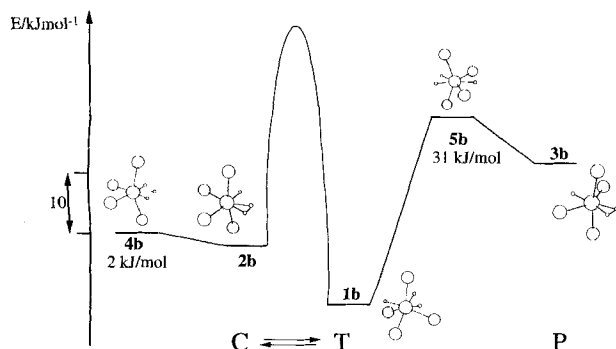


Figure 2. Relative energies of the T, C, and P isomers of  $[\text{Fe}(\text{PMe}_3)_4\text{H}_3]^+$ , together with activation barriers and possible transition states for hydrogen scrambling in the T and C structures.

ate in this exchange process. The structures **3b** and **5b** might further play a key role for the isomerization process  $\text{C}(\mathbf{2b}) \leftrightarrow \text{T}(\mathbf{1b})$ .<sup>[7]</sup>

We now return to the geometry of the transition-state structure **5b**. This molecule differs significantly from the T-type **1b** in all aspects. The angles P1–Fe–P2 and P3–Fe–P4 have opened up by 22.7° and 21.8°, respectively. The P1–Fe distance is 9 pm longer. With respect to the phosphorus ligand frame, **5b** is halfway in the transformation of **1b** to **3b**. But changes in the H coordination sphere are also observed. Besides the fact that H1 has moved between two P atoms, the distance H2–H3 is significantly reduced by 74 pm. The Fe center is now in the plane defined by H1, H2, and H3. The coordination of **5b** can be viewed as a distorted pentagonal bipyramid, or as a classical P<sub>c</sub>-type structure as discussed in the previous section. The structure of **5b** indeed bears similarities with the crystal structure obtained for the complex  $[\text{ReH}_3(\text{CO})(\text{PMe}_3)_3]$ .<sup>[24]</sup>

We close our discussion with an alternative view of the exchange process. Rather than describing **1b** as a seven-coordinate species, we choose a description based on eight-coordination.<sup>[26]</sup> The ligand framework of the T structure could be pictured as a distorted cube, in which one corner is unoccupied. The hydrogen exchange can then be described as a fluxional process involving rearrangement to a dodecahedron. The general motion for such a process is shown in Figure 3 a. The special rearrangement for the pathway **1b** ↔ **5b** is outlined in Figure 3 b.

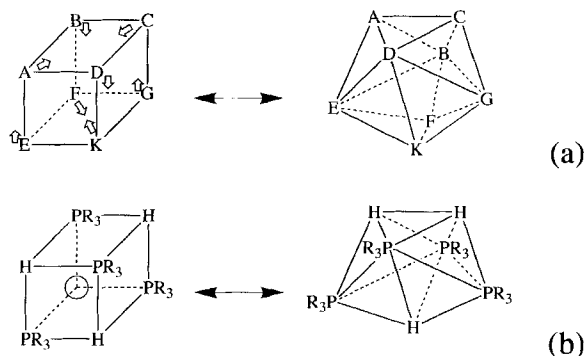


Figure 3. a) Dodecahedral distortion of a cube as b) a possible mechanism for hydrogen exchange in T- $[\text{Fe}(\text{PMe}_3)_4\text{H}_3]^+$ .

H2 and H3 occupy the positions A and B in the cube, and move toward each other during the process of dodecahedral distortion. H1 occupies the K position in the cube, and can be found in the dodecahedral structure on the average position between the former occupied K and the empty F position. In this way, the dodecahedral rearrangement leads from an eight-coordination situation to a seven-coordinated structure. The result again is a distorted pentagonal bipyramid or a classical P<sub>c</sub> structure, which is one of the basic geometries for seven-coordination.<sup>[26b, d]</sup> When arranging back to the cube, H1 can either move into the K or the F position. Thus, in the overall view, just one single ligand has effectively changed its place, in accordance with the tetrahedral jump model. The merit of this picture is that it stresses the synchronous participation of all ligands in the rearrangement process, rather than focusing on one particular kind of ligand.

## Concluding Remarks

In this study, we investigated structures, energetics and dynamics of the system  $[\text{Fe}(\text{PMe}_3)_4\text{H}_3]^+$ . We addressed the question of how well the  $\text{PMe}_3$  ligand is represented by the computationally less demanding model ligand  $\text{PH}_3$ . Concerning the geometries of various isomers of  $[\text{Fe}(\text{PR}_3)_4\text{H}_3]^+$ , we found that for both cases,  $\text{R} = \text{H}$  and  $\text{R} = \text{Me}$ , satisfactory structures were obtained in comparison with X-ray data. However, for an assessment of the relative energies of the isomers it is of paramount importance that the real ligand  $\text{PMe}_3$  is used in the calculations. We also investigated the hydrogen exchange in the C- and T-type isomers of  $[\text{Fe}(\text{PMe}_3)_4\text{H}_3]^+$ . For the C isomer, major movement of only the H ligands is required in the exchange process. For the T isomer, the mechanism might be described as a tetrahedral jump, but requires considerable movement of all the ligands in the coordination sphere around the metal center. Alternatively, we described this process as a dodecahedral distortion of a cubic arrangement. Further work on the isomers of the higher Group XIII homologues  $[\text{Ru}(\text{PMe}_3)_4\text{H}_3]^+$  and  $[\text{Os}(\text{PMe}_3)_4\text{H}_3]^+$ ,<sup>[29]</sup> as well as on the mechanism of the C $\leftrightarrow$ T isomerization process, is under way.

**Acknowledgments:** This work was supported by the Swiss National Science Foundation (SNSF). Access to the computing facilities of the Rechenzentrum der Universität Zürich is gratefully acknowledged.

Received: October 14, 1996 [F 495]

[1] E. L. Muetterties, *Acc. Chem. Res.* **1970**, *3*, 266.

[2] E. L. Muetterties, *Inorg. Chem.* **1965**, *4*, 769.

[3] a) F. N. Tebbe, P. Meakin, J. P. Jesson, E. L. Muetterties, *J. Am. Chem. Soc.* **1970**, *92*, 1068; b) P. Meakin, L. J. Guggenberger, J. P. Jesson, D. H. Gerlach, F. N. Tebbe, W. G. Peet, E. L. Muetterties, *ibid.* **1970**, *92*, 3482; c) P. Meakin, E. L. Muetterties, F. N. Tebbe, J. P. Jesson, *ibid.* **1971**, *93*, 4701; d) P. Meakin, E. L. Muetterties, J. P. Jesson, *ibid.* **1973**, *95*, 75.

[4] P. G. Jessop, R. H. Morris, *Coord. Chem. Rev.* **1992**, *121*, 155.

[5] For examples and references, see ref. [7].

[6] Initially, the term C-type structure was chosen to stress the *cis* arrangement of the H and  $\text{H}_2$  ligands, ref. [7].

[7] D. G. Gusev, R. Hübener, P. Burger, O. Orama, H. Berke, *J. Am. Chem. Soc.* **1997**, in press.

[8] a) T. Ziegler, *Pure. Appl. Chem.* **1991**, *28*, 1271; b) T. Ziegler, *Chem. Rev.* **1991**, *91*, 651; c) T. Ziegler, *Can. J. Chem.* **1995**, *73*, 743.

[9] For a compilation, see ref. [23a].

[10] Z. Lin, M. B. Hall, *J. Am. Chem. Soc.* **1992**, *114*, 2928.

[11] S. J. Vosko, M. Wilk, M. Nussair, *Can. J. Phys.* **1980**, *58*, 1200.

[12] a) A. Becke, *J. Chem. Phys.* **1986**, *84*, 4524; b) A. Becke, *ibid.* **1988**, *88*, 1053; c) A. Becke, *Phys. Rev.* **1988**, *A38*, 3098.

[13] a) J. P. Perdew, *Phys. Rev.* **1986**, *B33*, 8822; b) J. P. Perdew, *ibid.* **1986**, *B34*, 7406.

[14] a) E. J. Baerends, D. E. Ellis, P. E. Ros, *Chem. Phys.* **1973**, *2*, 41; b) G. teVelde, E. J. Baerends, *J. Comp. Phys.* **1992**, *99*, 84.

[15] a) E. J. Baerends, N. Rozendaal, *NATO Adv. Study Inst. Ser.* **1986**, *C176*, 159; b) T. Ziegler, *ibid.* **1991**, *C378*, 367.

[16] F. L. Hirshfeld, *Theor. Chim. Acta* **1977**, *44*, 129.

[17] a) F. Maseras, M. Duran, A. Lledós, J. Bertrán, *J. Am. Chem. Soc.* **1991**, *113*, 2879; b) F. Maseras, M. Duran, A. Lledós, J. Bertrán, *ibid.* **1992**, *114*, 2922.

[18] The difference in  $\sigma$  donor strength of  $\text{PMe}_3$  and  $\text{PH}_3$  can be analyzed in terms of Tolman's electronic parameter  $\chi$ , ref. [19]. The fact that the P atoms bear a higher positive charge in  $\text{PMe}_3$  complexes than in  $\text{PH}_3$  complexes (Table 3) supports the notion that the former ligand is the stronger  $\sigma$  donor.

[19] C. A. Tolman, *Chem. Rev.* **1977**, *77*, 313.

[20] Formal oxidation numbers and partial charges, obtained by quantum mechanical calculations, are both important but fundamentally different concepts, which have their advantages as well as limitations. For short comments and further literature, see ref. [21].

[21] a) M. Kaupp, H. G. v. Schnering, *Angew. Chem.* **1995**, *107*, 1076; *Angew. Chem. Int. Ed. Engl.* **1995**, *34*, 986; b) J. P. Snyder, *ibid.* **1995**, *107*, 1076 and **1995**, *34*, 986.

[22] a) G. J. Kubas, *Acc. Chem. Res.* **1988**, *21*, 120; b) G. J. Kubas, *Comments Inorg. Chem.* **1988**, *7*, 15.

[23] a) J. Li, R. M. Dickson, T. Ziegler, *J. Am. Chem. Soc.* **1995**, *117*, 11482; b) J. Li, T. Ziegler, *Organometallics* **1996**, *15*, 3844.

[24] D. G. Gusev, D. Nietlispach, I. L. Eremenko, H. Berke, *Inorg. Chem.* **1993**, *32*, 3628.

[25] Maseras and coworkers differentiate between two basic mechanisms of hydrogen exchange for **2a**, namely the open direct transfer and the addition-elimination mechanism. However, the latter mechanism, which is associated with an extremely high activation barrier of  $273 \text{ kJ mol}^{-1}$ , was established by fixing the angles  $-\text{H}-\text{Fe}-\text{H}$  at  $72^\circ$ , under the somewhat unreasonable assumption that all five equatorial ligands take on the angular arrangement of a regular pentagon. If this restriction is lifted, the two mechanisms mentioned above should become identical.

[26] For classical work on seven- and eight-coordination, compare ref. [27]. A good textbook treatment of molecular rearrangements can be found in ref. [28].

[27] a) J. L. Hoard, J. V. Silverton, *Inorg. Chem.* **1963**, *2*, 235; b) E. L. Muetterties, C. M. Wright, *Quart. Rev.* **1967**, *21*, 109; c) S. L. Lippard, *Prog. Inorg. Chem.* **1967**, *8*, 109; d) E. L. Muetterties, L. J. Guggenberger, *J. Am. Chem. Soc.* **1974**, *96*, 1748; e) J. K. Burdett, R. Hoffmann, R. C. Fay, *Inorg. Chem.* **1978**, *17*, 2553.

[28] K. F. Purcell, J. C. Kotz, *Inorganic Chemistry*, Holt-Saunders, Japan, **1985**, pp. 756.

[29] H. Jacobsen, H. Berke, unpublished results.